ISSN 1070-3284, Russian Journal of Coordination Chemistry, 2023, Vol. 49, No. 12, pp. 792–799. © Pleiades Publishing, Ltd., 2023.
Russian Text © The Author(s), 2023, published in Koordinatsionnaya Khimiya, 2023, Vol. 49, No. 12, pp. 752–759.

Mixed-Ligand Complex $[Cu_4(bpy)_4(PO_4)_2(CO_3)(H_2O)_2]$: Synthesis, Crystal Structure, and Biological Properties

K. A. Koshenskova[a], N. V. Makarenko[b, *], D. E. Baravikov[a], F. M. Dolgushin[a], O. B. Bekker[c], I. L. Eremenko[a], and I. A. Lutsenko[a, **]

[a] *Kurnakov Institute of General and Inorganic Chemistry, Russian Academy of Sciences, Moscow, Russia*
[b] *Institute of Chemistry, Far-Eastern Branch, Russian Academy of Sciences, Vladivostok, Russia*
[c] *Vavilov Institute of General Genetics, Russian Academy of Sciences, Moscow, Russia*
**e-mail: makarenko@ich.dvo.ru*
***e-mail: irinalu05@rambler.ru*

Received May 19, 2023; revised July 23, 2023; accepted July 24, 2023

Abstract—The reactions in the $Cu(OAc)_2 \cdot H_2O$–phytic acid–2,2'-bipyridine (bpy) system in aqueous methanol solutions resulted in the formation of a molecular different-ligand tetranuclear complex $[(Cu_4(bpy)_4(PO_4)_2(CO_3)(H_2O)_2] \cdot 13H_2O$ (**I**), the structure of which was established from the X-ray diffraction data (CCDC no. 2262998). The molecule of complex **I** contains four non-equivalent Cu^{2+} cations, coordinating each two phosphate anions (PO_4^{3-} remaining after the transformation of the phytate ring), four neutral bpy molecules, two water molecules, and one carbonate anion (CO_3^{2-}). The presence of a large number of solvate water molecules in the outer coordination sphere gives rise to a hydrogen-bonded framework involved in stabilization of the crystal packing. Study of the antimycobacterial activity of **I** against non-pathogenic *Mycolicibacterium smegmatis* strain revealed high biological efficacy.

Keywords: copper(II), coordination compound, synthesis, crystal structure, biological activity, *Mycolicibacterium smegmatis*

DOI: 10.1134/S1070328423601073

INTRODUCTION

Coordination compounds based on essential (vital) metals are in a relevant field of research for medicinal, bioinorganic, and pharmaceutical chemistry, related to the possibility of forming structures that exhibit various biological activities. For example, platinum complexes possess antiproliferative activity; gold is a part of anti-arthritis drugs; and zinc, silver, and mercury have antimicrobial properties [1–6]. A promising complex-forming metal (perhaps, an alternative to platinum) is copper, which performs a number of vital redox functions in the cell, e.g., transport of the respiratory chain electrons, oxidative phosphorylation, removal of superoxide radicals, etc. [7–9]. A number of studies attest to various types of biological activity of copper(II) complexes: antiblastic (antiproliferative), antimicrobial, antimycobacterial, and other activities [10–19]. The ligands used most often for the formation of biologically active complexes are various carboxylate ligands (which, furthermore, provide for the solubility of compounds), while oligo- and polypyridine moieties such as phenanthrolines, bipyridines, and terpyridines are employed for increasing the bioefficacy [20–24].

In the present study, phytic acid (inositol hexaphosphoric acid, $C_6H_6[OPO(OH)_2]_6$) was used as the acidic molecule. Phytic acid is a typical plant-derived product [25–28], the pharmacophore moiety of which is vitamin B8 synthesized by intestinal cells. The reactivity of phytic acid is due to the presence of active protons in the molecule (Scheme 1), while the six-membered ring enables the existence of various isomers [29–31].

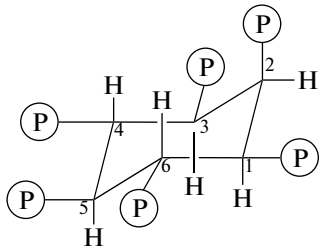

Scheme 1.

Phytic acid chelates especially actively divalent metal ions (Cu^{2+}, Mn^{2+}, Zn^{2+}) [32–35]. According to X-ray diffraction data, in the Cu(II)–phytate–L sys-

tems (L = terpyridine, 1,10-phenanthroline), each copper(II) cation coordinates N-donor ligands in the bi- and tridentate fashion, while the phytate anion binds via one or two PO_4^{3-} groups [32].

The purpose of the present study is to develop a procedure for the synthesis in the Cu(II)–$C_6H_6[OPO(OH)_2]_6$–bpy system (bpy = 2,2'-bipyridine), establish the product structure by X-ray diffraction, and determine the biological activity against the model non-pathogenic *Mycolicibacterium smegmatis* strain.

EXPERIMENTAL

Complex **I** was synthesized in air using distilled water, methanol (reagent grade, Khimmed), and ethanol (reagent grade, Khimmed) and commercially available chemicals: sodium phytate hydrate $C_6H_{18}O_{24}P_6{\cdot}x\mathrm{Na}{\cdot}yH_2O$ (Sigma Aldrich), copper(II) acetate monohydrate $(Cu(OAc)_2{\cdot}H_2O$ (95%, Acros), bpy (reagent grade, Khimmed), and tetra-*n*-butylammonium hydroxide (Bu_4NOH 40% aqueous solution, Alfa Aesar).

Elemental analysis was carried out on a Carlo Erba EA 1108 automatic C,H,N-analyzer.

IR spectra were recorded on a Perkin-Elmer Spectrum 65 FTIR spectrophotometer by the attenuated total reflectance (ATR) method in the 400–4000 cm^{-1} frequency range.

The biological activity of compound **I** was assessed using the *M. smegmatis* mc^2 155 strain by the disc diffusion assay. The growth inhibition zone was measured for the strain inoculated as a lawn on an agar medium around paper discs containing the test compound in various concentrations. The bacteria washed from the Petri dishes with the Tryptone soya agar M-290 (Himedia) were grown overnight in the Lemco-TW liquid medium (Lab Lemco' Powder, 5 g L^{-1} (Oxoid); Peptone special, 5 g L^{-1} (Oxoid); NaCl, 5 g L^{-1}, Tween-80) at 37°C up to the mid-logarithmic growth phase (OD_{600} = 1.5) and mixed with molten agar M-290 medium in 1 : 9 : 10 ratio (culture : Lemco-TW : M-290). The culture was incubated for 24 h at 37°C. The compound concentration that induced the minimum growth inhibition zone for mycobacteria was taken as the minimum inhibitory concentration (MIC).

Synthesis of $[Cu_4(bpy)_4(PO_4)_2(CO_3)(H_2O)_2]{\cdot}13H_2O$ (I). A weighed portion of sodium phytate $C_6H_{18}O_{24}P_6{\cdot}x\mathrm{Na}{\cdot}yH_2O$ (0.165 g, 0.25 mmol) was dissolved in H_2O (10 mL), Bu_4NOH (2 mL) was added, and the mixture was kept at room temperature for 30 min. Then $Cu(OAc)_2{\cdot}H_2O$ (0.100 g, 0.5 mmol) and bpy (0.078 g, 0.5 mmol) dissolved in MeOH (15 mL) were added to the resulting solution. The reaction mixture was kept at 60°C for 90 min, and the resulting light blue solution was filtered. After a week, a light blue polycrystalline material was formed on the bottom of the flask; the precipitate was separated from the mother liquor by decantation. The crystals suitable for X-ray diffraction were obtained by recrystallization of the product from a EtOH : H_2O mixture (1 : 1). The yield of **I** was 0.079 g (45%).

For $C_{41}H_{62}N_8O_{26}P_2Cu_4$ (**I**)			
Anal. calcd., %	C, 35.20	H, 4.47	N, 8.01
Found, %	C, 35.22	H, 4.33	N, 7.89

IR (ν, cm^{-1}): 3205 br.m, 3111 m, 3078 br.m, 2346 w, 2041 vw, 1907 vw, 1604 m, 1551 m, 1489 m, 1473 m, 1442 s, 1317 m, 1251 m, 1159 m, 1070 s, 993 vs, 857 s, 767 vs, 727 s, 586 vs, 547 vs, 414 vs.

X-ray diffraction study of complex **I** was carried out at 100 K on a Bruker Apex II diffractometer (CCD array detector, MoK_α radiation, λ = 0.71073 Å, graphite monochromator). The structure was solved using the ShelXT program [36] and refined by the full-matrix least-squares method with the Olex2 program [37] in the anisotropic approximation for non-hydrogen atoms. For the water molecules of crystallization not coordinated to the complex, 19 sites were located in the difference maps; some of these sites were partly occupied. The total occupancy for the water molecules of crystallization was 13 according to X-ray diffraction data. The hydrogen atoms of water molecules were located from difference Fourier maps, and the positions of the other hydrogen atoms were calculated geometrically. All of them were refined in the isotropic approximation using the riding model. The main crystallographic data and refinement parameters were as follows: $C_{41}H_{62}N_8O_{26}P_2Cu_4$, M = 1388.08 g/mol, monoclinic space group $P2/c$, a = 14.1175(6), b = 18.5107(8), c = 21.5449(9) Å, β = 94.404(2)°, V = 5546.2(4) $Å^3$, ρ(calcd.) = 1.666 g/cm^3, Z = 4, scanning angle 3.664° < 2θ < 50.5°, μ(Mo) = 1.662 mm^{-1}, 91398 reflections were measured, 10027 reflections were unique, and 7755 of these reflections had $I > 2\sigma(I)$; R_{int} = 0.1046, R_1 = 0.0562, and wR_2 = 0.1349 for the observed reflections with $I > 2\sigma(I)$, and R_1 = 0.0778 and wR_2 = 0.1502 for all reflections; the number of refined parameters was 790.

The full set of X-ray diffraction data was deposited with the Cambridge Crystallographic Data Centre (CCDC no. 2262998; deposit@ccdc.cam.uk).

RESULTS AND DISCUSSION

Compound **I** crystallizes in monoclinic space group $P2/c$ and represents a solvated different-ligand tetranuclear molecular complex $[(Cu_4(bpy)_4(PO_4)^2\text{-}(CO_3)(H_2O)_2]{\cdot}13H_2O$ (Fig. 1). Unlike the previously reported Cu(II) complexes with phytic acid in which a

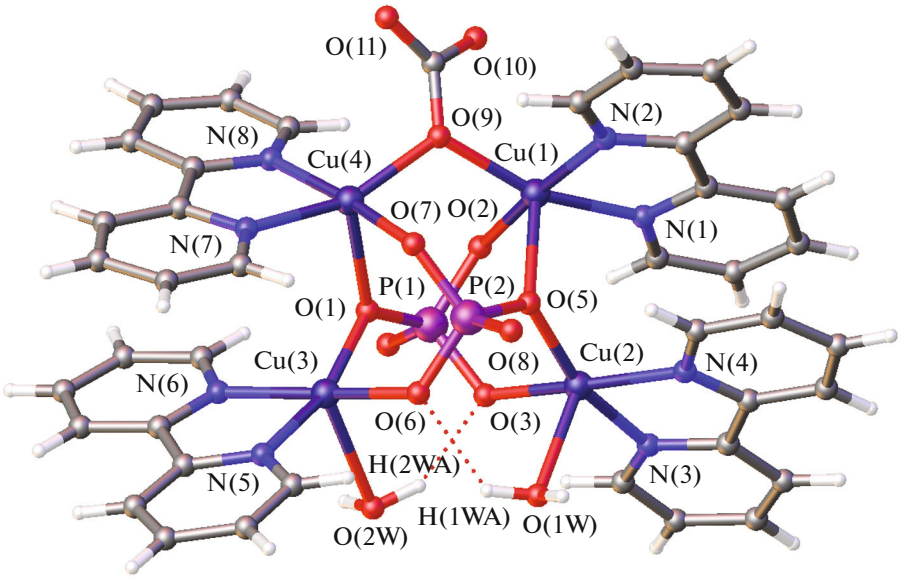

Fig. 1. Molecular structure of **I**. The dashed lines designate hydrogen bonds.

pair of inositol moieties is coordinated to the metal via the PO_4^{3-} anion [33, 34], in our case, the molecule contains four non-equivalent Cu^{2+} cations, coordinating two phosphate anions (PO_4^{3-} anions remaining after transformation of the phytate ring), four neutral bpy molecules, two water molecules, and a carbonate anion moiety (CO_3^{2-}). Each copper atom occurs in a square pyramidal environment of nitrogen and oxygen atoms $\{CuN_2O_3\}$ (coordination number 5). In terms of the coordination environment, the complex-forming atoms can be divided into two groups: the first group atoms (Cu(1), Cu(4)) are chelated by bpy (Cu–N, 1.996(5)–2.024(5) Å) and are bound to a carbonate anion (Cu–O, 1.945(4); 1.951(4) Å) and two phosphate anions (Cu–O, 1.923(4)–2.288(4) Å), while the second group atoms (Cu(2), Cu(3)) are chelated by bpy (Cu–N, 2.000(6)–2.022(5) Å) and are bound to two phosphate anions (Cu–O, 1.927(4)–1.942(4) Å) and water molecules (Cu(2)–O(1*w*), 2.294(4); Cu(3)–O(2*w*), 2.328(4) Å) (Table 1).

Also, in compound **I**, intramolecular hydrogen bonds are formed between the coordinated water molecules and phosphoric acid residues (O(1*w*)–H(1*w*A)...O(6), 2.057 Å; O(1*w*)...O(6), 2.719(5) Å; O(2*w*)–H(2*w*A)...O(3), 1.985 Å; and O(2*w*)...O(3), 2.785(5) Å) (Fig. 1).

The crystal packing is stabilized by numerous hydrogen bonds involving outer-sphere water molecules (13 positions of water molecules were identified in the independent part of the unit cell), which give rise to a structure-forming hydrogen-bonded layer (Fig. 2, Table 2). The presence of a large number of hydration molecules in the crystal packing determines a good water solubility of the compound, which is a necessary condition for the development of drug candidates.

There are weak π-stacking interactions between the bipyridine moieties of the neighboring molecules (rings 1: N(1)C(1)C(2)C(3)C(4)C(5); 2: N(2)C(6)-C(7)C(8)C(9)C(10); 3: N(1)C(1)C(2)C(3)C(4)-$C(5)_{1-x,\,1-y,\,1-z}$; 4: $N(2)C(6)C(7)C(8)C(9)C(10)_{1-x,\,1-y,\,1-z}$; 5: N(7)C(31)C(32)C(33)C(34)C(35); 6: N(8)C(36)-C(37)C(38)C(39)C(40); 7: $N(7)C(31)C(32)C(33)-C(34)C(35)_{1-x,\ -y,\ 1-z}$; 8: $N(8)C(36)C(37)C(38)-C(39)C(40)_{1-x,\,-y,\,1-z}$; 1–4, 2–3 = 3.613 Å; 5–8, 6–7 = 3.690 Å). Finally, the layers are bound into a single 3D structure (Fig. 3).

The antibacterial activity of compound **I** was determined against the non-pathogenic *M. smegmatis* strain, which is a model for the virulent *Mycobacterium tuberculosis*. It is known that the resistance of mycobacteria to chemotherapeutic agents is largely related to low permeability and unusual structure of the mycobacterial cell wall. *M. smegmatis* is a fast-growing non-pathogenic bacterium and, hence, it is used to model the slowly growing *M. tuberculosis* bacterium and for the primary screening of antituberculosis drugs [38]. The *M. smegmatis* strain is more resistant to antibiotics and antituberculosis agents than *M. tuberculosis*, therefore, the concentration <100 μmol/disc was used as the selection criterion [39]. The obtained results on the in vitro biological activity for the test compounds were compared with the activities of isoniazid (INH) and rifampicin (Rif), used as the first-line drugs for the antituberculosis therapy, under the same experimental conditions.

The data on the antibacterial activity in the *M. smegmatis* mc^2 155 test system and its variation with time for compound **I** are summarized in Table 3.

Table 1. Selected bond lengths (*d*, Å) in **I**

Bond	*d*, Å	Bond	*d*, Å
bpy			
Cu(1)–N(1)	2.024(5)	Cu(3)–N(5)	2.004(4)
Cu(1)–N(2)	1.996(5)	Cu(3)–N(6)	2.002(5)
Cu(2)–N(3)	2.008(4)	Cu(4)–N(7)	2.022(5)
Cu(2)–N(4)	2.007(4)	Cu(4)–N(8)	2.000(6)
PO_4^{3-}			
Cu(1)–O(2)	1.929(4)	Cu(3)–O(1)	1.942(4)
Cu(1)–O(5)	2.283(4)	Cu(3)–O(6)	1.927(4)
Cu(2)–O(3)	1.941(4)	Cu(4)–O(1)	2.288(4)
Cu(2)–O(5)	1.942(3)	Cu(4)–O(7)	1.923(4)
CO_3^{2-}			
Cu(1)–O(9)	1.951(4)	Cu(4)–O(9)	1.945(4)
H_2O			
Cu(2)–O(1)	2.294(4)	Cu(3)–O(2*w*)	2.328(4)
Cu...Cu			
Cu(1)...Cu(4)	3.328(1)	Cu(1)...Cu(2)	3.301(2)
Cu(2)...Cu(3)	4.295(3)	Cu(3)...Cu(4)	3.252(2)

In terms of MIC, the obtained copper complex is more active than the ligands by a factor of several tens (>10 times more active than $C_6H_{18}O_{24}P_6{\cdot}x\mathrm{Na}{\cdot}yH_2O$ and 20 times more active than bpy). It is four times more active than isoniazid, but is inferior to rifampicin. As follows from Table 3, the bioactivity of free organic ligands is, on the one hand, low and, on the other hand, short-term (the inhibition zone of mycobacterial growth is overgrown within the first 24 h). Upon complex formation, the effect becomes more lengthy: the growth inhibition zone is retained for almost 5 days. In comparison with the previously synthesized copper(II) furancarboxylate complexes, compound **I** can be placed in the series of increasing bioactivity between the pyridine and phenanthroline compounds [15, 16, 18, 19, 40–42]. Among bipyridine complexes with various metals (copper(II), zinc(II), nickel(II), cobalt(II)), compound **I** is one of the most active, being inferior only to $[Cu_2(Nfur)_4(bpy)_2]{\cdot}H_2O$ [19] (MIC = 20 nmol/disc; Table 3). An interesting

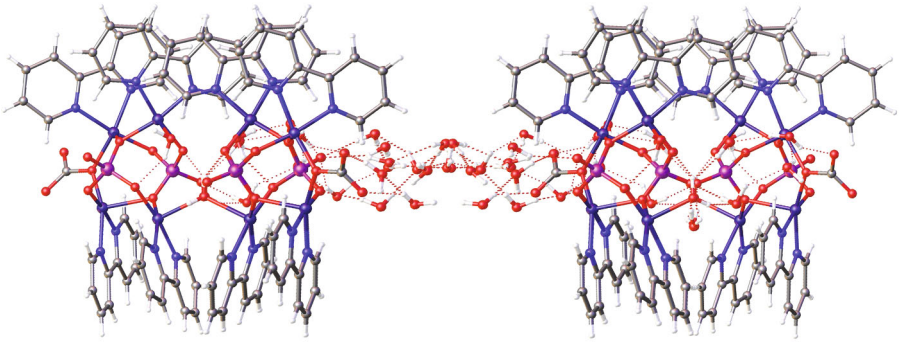

Fig. 2. Formation of the hydrogen-bonded framework.

Table 2. Geometric parameters of hydrogen bonds in **I***

D–H...A	Distances, Å			D–H...A angle, deg
	D–H	H...A	D...A	
O(1*w*)–H(1*w*A)...O(6)	0.87	2.06	2.719(5)	132.3
O(1*w*)–H(1*w*B)...O(11*w*)	0.87	1.92	2.742(6)	156.6
O(2*w*) –H(2*w*A)...O(3)	0.87	1.99	2.785(5)	152.2
O(2*w*)–H(2*w*B)...O(3*w*)	0.87	1.94	2.796(6)	166.6
O(3*w*)–H(3*w*A)...O(4)	0.87	1.87	2.718(6)	164.5
O(3*w*)–H(3*w*B)...O(4*w*)	0.86	1.90	2.698(7)	154.4
O(4*w*)–H(4*w*A)...O(5*w*)	0.87	1.99	2.778(8)	149.4
O(4*w*)–H(4*w*B)...O(18*w*)	0.87	1.86	2.661(8)	151.5
O(5*w*)–H(5*w*A)...O(7*w*)	0.87	1.90	2.724(10)	157.5
O(5*w*)–H(5*w*B)...O(4)	0.87	1.97	2.775(6)	153.8
O(6*w*)–H(6*w*B)...O(4)	0.87	1.77	2.621(9)	165.6
O(7*w*)–H(7*w*A)...O(16*w*)	0.87	1.96	2.725(10)	146.0
O(7*w*)–H(7*w*B)...O(8*w*)$^{1\#}$	0.87	2.13	2.764(17)	128.8
O(7*w*)–H(7*w*B)...O(8*w*)	0.87	2.04	2.865(16)	159.2
O(8*w*)–H(8*w*B)...O(9*w*)	0.94	2.14	2.748(16)	121.5
O(9*w*)–H(9*w*A)...O(19*w*)	0.87	1.83	2.555(17)	140.1
O(9*w*)–H(9*w*B)...O(6*w*)	0.87	1.89	2.676(15)	150.4
O(10*w*)–H(10A)...O(9*w*)	0.87	1.82	2.685(10)	175.8
O(10*w*)–H(10B)...O(2)	0.87	1.87	2.730(6)	169.4
O(11*w*)–H(11A)...O(8)	0.87	1.84	2.694(6)	169.2
O(11*w*)–H(11B)...O(4*w*)$^{2\#}$	0.87	2.03	2.712(8)	134.9
O(12*w*)–H(12A)...O(8)	0.87	1.91	2.774(6)	174.8
O(12*w*)–H(12B)...O(7)$^{3\#}$	0.87	1.95	2.795(6)	162.3
O(13*w*)–H(13A)...O(8)	0.87	1.96	2.805(5)	164.2
O(13*w*)–H(13B)...O(83)	0.87	2.09	2.805(5)	138.7
O(14*w*)–H(14A)...O(10)	0.87	1.82	2.494(16)	132.7
O(14*w*)–H(14A)...O(15*w*)$^{4\#}$	0.87	1.89	2.76(2)	173.1
O(15*w*)–H(15B)...O(11)$^{5\#}$	0.87	1.04	1.88(2)	157.5
O(16*w*)–H(16A)...O(15*w*)	0.87	1.38	2.20(2)	155.4
O(18*w*)–H(18A)...O(11)$^{5\#}$	0.87	1.84	2.645(10)	152.8
O(18*w*)–H(18B)...O(12*w*)$^{2\#}$	0.87	1.86	2.697(8)	162.2
O(19*w*)–H(19A)...O(16*w*)$^{1\#}$	0.87	2.14	2.839(15)	137.1
O(19*w*)–H(19B)...O(17*w*)$^{6\#}$	0.83	1.63	2.44(3)	167.0
O(21*w*)–H(21B)...O(4)	0.87	2.15	2.85(3)	136.9

* Symmetry codes: $^{1\#}$ $-x, y, 3/2 - z$; $^{2\#}$ $-x, y, 1/2 - z$; $^{3\#}$ $1 - x, y, 1/2 - z$; $^{4\#}$ $1 + x, y, z$; $^{5\#}$ $-1 + x, y, z$; $^{6\#}$ $1 - x, y, 3/2 - z$.

Table 3. Antibacterial activity assays in vitro for **I** against *Mycolicibacterium smegmatis*

Compound*	MIC, nmol/disc	Inhibition zone, mm		Ref.
	24 h	24 h	120 h	
I	25	6.6 ± 0.1	6.5 ± 0.1	This work
$[Cu(Fur)_2(phen)]$	5	7 ± 0.5	7 ± 0.5	[15]
$[Cu_2(Fur)_4(Py)_2]$	200	7 ± 0.5	7 ± 0.5*	[15]
$[Cu(Fur)_2(Py)_2(H_2O)]$	400	7 ± 0.5	7 ± 0.5*	[15]
$[Cu(Fur)_2(bpy)(H_2O)]$	100	7.0 ± 0.5	7.0 ± 0.5*	[16]
$[Cu(Fur)_2(Phpy)_2(H_2O)]\cdot Phpy$	250	7.0 ± 0.5	7.0 ± 0.5*	[40]
$[Cu(Fur)_2(NH_2\text{-}Py)_2]$	1000	7.0 ± 0.5	7.0 ± 0.5*	[40]
$[Cu_2(Fur)_4(CH_3CN)_2]$	187	7.0 ± 0.5	7.0 ± 0.5*	[41]
$[Cu(Fur)_2Neoc(H_2O)]$	25	6.7 ± 0.3	6.6 ± 0.1	[18]
$[Cu(Nfur)_2(H_2O)_2]\cdot 2H_2O$	1000	6.7 ± 0.1	6.4 ± 0.1*	[19]
$[Cu(Nfur)_2(Py)_2(H_2O)]$	800	6.8 ± 0.3	6.6 ± 0*	[19]
$[Cu_2(Nfur)_4(bpy)_2]\cdot H_2O$	20	7.0 ± 0.0	6.9 ± 0.1*	[19]
$[Zn(Fur)_2(bpy)]$	100	6.5 ± 0.0	0	[16]
$[Co(Fur)_2(bpy)]$	400	6.5 ± 0.2	6.5 ± 0.2*	[16]
$[Ni(Fur)_2(bpy)]$	>2000	6.6 ± 0.12	6.5 ± 0.1*	[42]
$C_6H_{18}O_{24}P_6\cdot x Na\cdot y H_2O$	>250	0	0	This work
2HFur	1000	6.5 ± 0.2	0	[15]
HNfur	>1000	0	0	[19]
phen	45	7.5 ± 0.5	0	[18]
Neoc	100	6.46 ± 0.06	0	[18]
bpy	500	0	0	[16]
INH	100	7 ± 0.5	6.5 ± 0.5	This work
Rif	5	7.2 ± 0.3	7.0 ± 0	This work

phen is 1,10-phenanthroline, Phpy is 4-phenylpyridine, NH_2-Py is 3-aminopyridine, Neoc is 2,9-dimethyl-1,10-phenanthroline (neocuproine), $C_6H_{18}O_{24}P_6\cdot x Na\cdot y H_2O$ is sodium phytate hydrate, bpy is 2,2'-bipyridine, INH is isoniazid, Rif is rifampicin, HFur and Nfur are 2-furanoic and 5-nitro-2-furanoic acids.
* The growth inhibition zone of the bacterial culture, which initially appeared after a few hours of growth, begins to be overgrown over the entire surface of the zone.
0 means that no growth inhibition zone.

feature of **I** was noted during the experiment; unlike the binuclear complex obtained previously [19], compound **I** has a bactericidal effect, i.e., the bacterial growth inhibition zone is not overgrown after 120 h.

ACKNOWLEDGMENTS

X-ray diffraction studies, elemental analysis, and IR spectroscopy were performed using equipment of the Center for Collective Use of Physical Investigation Methods of the Kurnakov Institute of General and Inorganic Chemistry, Russian Academy of Sciences.

FUNDING

This study was performed within the framework of the state assignment for the Kurnakov Institute of General and Inorganic Chemistry, Russian Academy of Sciences in the field of scientific research, programs of the Russian Academy of Sciences, and state assignment for the Institute of Chemistry, Far-Eastern Branch, Russian Academy of Sciences FWFN(0205)-2022-0003.

CONFLICT OF INTEREST

The authors of this work declare that they have no conflicts of interest.

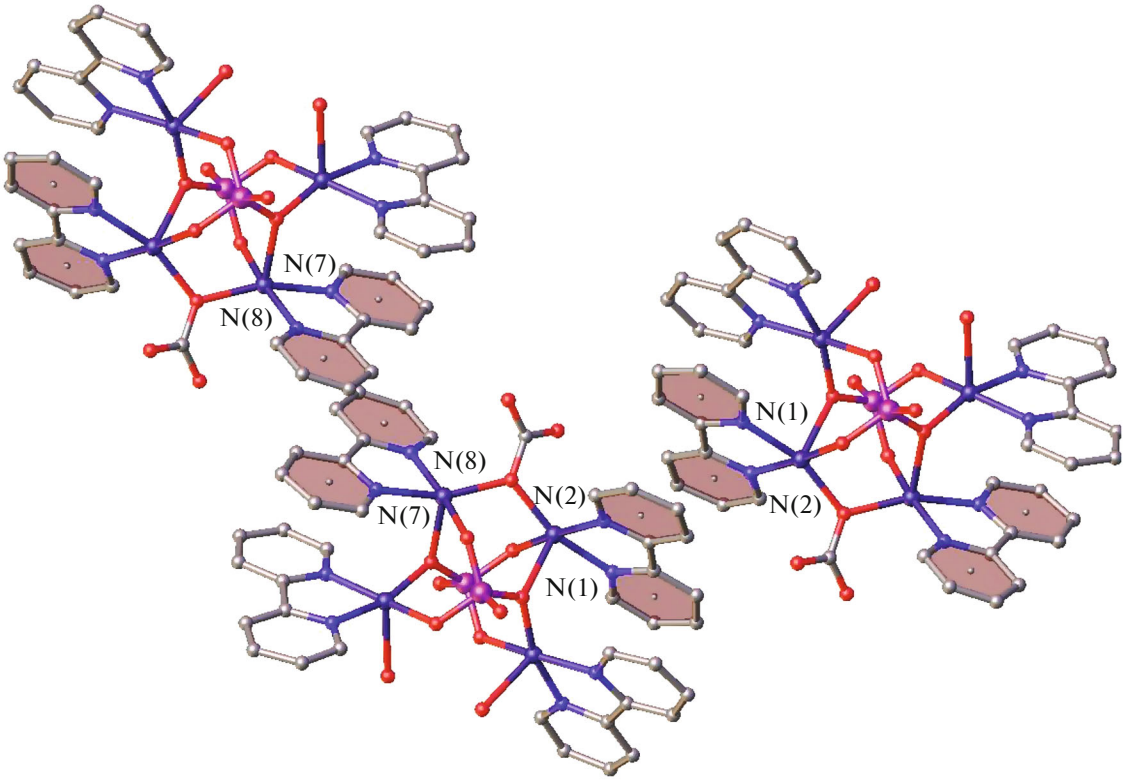

Fig. 3. π-Stacking interactions between the bpy moieties in **I**.

REFERENCES

1. Barry, N. and Sadler, P., *Chem. Commun.*, 2013, vol. 49, p. 5106.
2. Chan, W. and Wong, W., *Polyhedron*, 2014, vol. 83, p. 150.
3. Medici, S., Peana, M., Nurchi, V., et al., *Coord. Chem. Rev.*, 2015, vol. 284, p. 329.
4. Che, C.-M. and Siu, F.-M., *Curr. Opin. Chem. Biol.*, 2010, vol. 14, p. 255.
5. Dilruba, S. and Kalayda, G.V., *Cancer Chemother. Pharmacol.*, 2016, vol. 77, p. 1103.
6. Porchia, M., Pellei, M., Del Bello, F., et al., *Molecules*, 2020, vol. 25, p. 5814.
7. Linder, M.C. and Hazegh-Azam, M., *Am. J. Clin. Nutr.*, 1996, vol. 63, p. 797.
8. Kaim, W. and Rall, J., *Angew. Chem., Int. Ed. Engl.*, 1996, vol. 35, p. 43.
9. Crichton, R.R. and Pierre, J.-L., *Biometals*, 2001, vol. 14, p. 99.
10. Climova, A., Pivovarova, E., Szczesio, M., et al., *J. Inorg. Biochem.*, 2023, vol. 240, p. 112108.
11. Gordon, A.T., Abosede, O., Ntsimango, S., et al., *Inorg. Chim. Acta*, 2020, vol. 510, p. 119744.
12. Bravo-Gómez, M., Campero-Peredo, C., García-Conde, D., et al., *Polyhedron*, 2015, vol. 102, p. 530.
13. Davila-Manzanilla, S., Figueroa-de-Paz, Y., Mejia, C., et al., *Eur. J. Med. Chem.*, 2017, vol. 129, p. 266.
14. Correia, I., Borovic, S., Cavaco, I., et al., *J. Inorg. Biochem.*, 2017, vol. 175, p. 284.
15. Lutsenko, I.A., Baravikov, D.E., Kiskin, M.A., et al., *Russ. J. Coord. Chem.*, 2020, vol. 46, no. 6, p. 411. https://doi.org/10.1134/S1070328420060056
16. Lutsenko, I.A., Yambulatov, D.S., Kiskin, M.A., et al., *Russ. J. Coord. Chem.*, 2020, vol. 46, no. 12, p. 787. https://doi.org/10.1134/S1070328420120040
17. Lutsenko, I.A., Yambulatov, D.S., Kiskin, M.A., et al., *Chem. Select.*, 2020, vol. 5, p. 11837.
18. Lutsenko, I.A., Baravikov, D.E., Koshenskova, K.A., et al., *RSC Advances*, 2022, vol. 12, p. 5173.
19. Koshenskova, K.A., Lutsenko, I.A., Nelyubina, Yu.V., et al., *Russ. J. Inorg. Chem.*, 2022, vol. 67, p. 1545. https://doi.org/10.31857/S0044457X22700106
20. Naletova, I., Satriano, K., Cursi, A., et al., *Oncotarget*, 2018, vol. 9, p. 36289.
21. Pivetta, T., Trudu, F., Valletta, E., et al., *J. Inorg. Biochem.*, 2014, vol. 141, p. 103.
22. Koshenskova, K.A., Baravikov, D.E., Nelyubina, Yu.V., et al., *Russ. J. Coord. Chem.*, 2023, vol. 49, no. 10, p. 660.
23. Eremina, J.A., Lider, E.V., Kuratieva, N.V., et al., *Inorg. Chim. Acta*, 2021, vol. 516, p. 120169. https://doi.org/10.1134/S1070328423600730
24. Eremina, J.A., Smirnova, K.S., Berezin, A.S., et al., *J. Mol. Struct.*, 2021, vol. 1245, p. 131024.
25. Saburov, K.A. and Kamilov, Kh.M., *Chem. Nat. Compd.*, 1989, vol. 25, no. 6, p. 695.

26. Barrientos, L.G. and Murthy, P.P.N., *Carbohydr. Res.*, 1996, vol. 296, p. 39.
27. Raboy, V., *Phytochemistry*, 2003, vol. 64, no. 6, p. 1033.
28. Vasca, E., Materazzi, S., Caruso, T., et al., *Anal. Bioanal. Chem. Res.*, 2002, vol. 374, no. 1, p. 173.
29. Stefano, C.De., Giuffre, O., Milea, D., et al., *Chem. Spec. Bioavail.*, 2002, vol. 15, no. 2, p. 29.
30. Yu, S., Cowieson, A., Gilbert, C., et al., *J. Anim. Sci.*, 2012, vol. 90, p. 1824.
31. Nielsen, A.V.F., Tetens, I., and Meyer, A.S., *Nutrients*, 2013, vol. 5, p. 3074.
32. Veiga, N., Torres, J., Bazzicalupi, C., et al., *Chem. Commun.*, 2014, vol. 50, p. 14971.
33. Quiñone, D., Veiga, N., Torres, J., et al., *Dalton Trans.*, 2016, vol. 45, p. 12156.
34. Quiñone, D., Veiga, N., Torres, J., et al., *ChemPlusChem.*, 2017, vol. 82, no. 5, p. 721.
35. Cai, K., Sun, F., Liang, X., et al., *J. Mater. Chem. A*, 2017, vol. 5, p. 12943.
36. Sheldrick, G.M., *Acta Crystallogr., Sect. A: Found. Adv.*, 2015, vol. 71, p. 3.
37. Dolomanov, O.V., Bourhis, L.J., Gildea, R.J., et al., *J. Appl. Crystallogr.*, 2009, vol. 42, p. 339.
38. Ramon-García, S., Ng, C., Anderson, H., et al., *Antimicrob. Agents Chemother.*, 2011, vol. 8, p. 3861.
39. Bekker, O.B., Sokolov, D.N., Luzina, O.A., et al., *Med. Chem. Res.*, 2015, vol. 24, p. 2926.
40. Lutsenko, I.A., Kiskin, M.A., Koshenskova, K.A., et al., *Russ. Chem. Bull.*, 2021, vol. 70, no. 3, p. 463. https://doi.org/10.1007/s11172-021-3109-3
41. Lutsenko, I.A., Nikiforova, M.E., Koshenskova, K.A., et al., *Russ. J. Coord. Chem.*, 2021, vol. 47, no. 12, p. 879. https://doi.org/10.31857/S0132344X22020049
42. Uvarova, M.A., Lutsenko, I.A., Kiskin, M.A., et al., *Polyhedron*, 2021, vol. 203, p. 115241.

Translated by Z. Svitanko